

The Magnetic Field of the Large Magellanic Cloud: A New Way of Studying Galactic Magnetism

Bryan M. Gaensler^{*†}, M. Haverkorn^{*}, L. Staveley-Smith[‡], J. M. Dickey[§],
N. M. McClure-Griffiths[‡], J. R. Dickel[¶] and M. Wolleben^{||}

Abstract

We present a study of the Faraday rotation of extragalactic sources lying behind the Large Magellanic Cloud. These data represent the most detailed study yet of magnetic field structures in any external galaxy, and are a demonstration of how magnetic fields in galaxies will best be studied with future instruments.

1 Introduction

The Large Magellanic Cloud (LMC) is the prototype of the barred Magellanic spiral class of galaxies, and shows spectacular evidence for on-going interaction with both the Milky Way and the Small Magellanic Cloud (SMC). The LMC's proximity, low inclination, and minimal foreground and internal extinction all make it an ideal target for studying both specific populations and overall galactic structure. There have correspondingly been many recent detailed studies of stars, gas and dust in the LMC, but surprisingly little is known about this galaxy's magnetic fields. Here we summarise previous work on the LMC's magnetism, present a new study of the LMC using background rotation measures (RMs) (see Gaensler et al. 2005 for further discussion), and explain how this technique can be applied to this and other galaxies in future studies (for a review see Gaensler et al. 2004 and Beck & Gaensler 2004).

2 Previous Studies of the LMC's Magnetism

The earliest studies of magnetic fields in the LMC were carried out through the study of polarisation of optical starlight (e.g., Visvanathan 1966; Mathewson & Ford 1970; Schmidt 1976). These data suggested the presence of a possible spiral field geometry in the vicinity of the star-forming region 30 Doradus, plus the overall presence of a "pan-Magellanic field", directed along a line joining the LMC to the SMC (see Wayte 1990 for a summary).

The strength of the LMC's magnetic field can be estimated through observations of its diffuse radio synchrotron emission: standard equipartition arguments imply a mean field strength of $\approx 6 \mu\text{G}$ (Klein et al. 1989), a value supported by γ -ray observations which allow a direct separation of energy in particles and in magnetic fields (Pohl 1993, but see also Chi & Wolfendale 1993). Additionally, one LMC pulsar (PSR B0529-66) has a measured RM, implying a line-of-sight field strength in the range $0.5\text{--}2 \mu\text{G}$ (Costa et al. 1991).

^{*}Harvard-Smithsonian Center for Astrophysics, 60 Garden Street MS-6, Cambridge, MA 02138, USA

[†]School of Physics, University of Sydney, NSW 2006, Australia

[‡]Australia Telescope National Facility, CSIRO, PO Box 76, Epping, NSW 1710, Australia

[§]Physics Department, University of Tasmania, GPO Box 252-21, Hobart, Tasmania 7001, Australia

[¶]Astronomy Department, University of Illinois, 1002 West Green Street, Urbana, IL 61801, USA

^{||}Max-Planck-Institut für Radioastronomie, Auf dem Hügel 69, D-53121 Bonn, Germany

Direct imaging of the polarised synchrotron emission from the LMC provides further clues as to this galaxy’s magnetic field geometry. Such imaging was carried out with the Parkes radio telescope by Klein et al. (1993), revealing a polarised morphology which was dominated by two highly polarised “fingers” of emission to the south of 30 Dor, as shown in Figure 1(a). Klein et al. (1993) suggested that these might trace a magnetic loop, extending out of the LMC’s disk.

The vectors of polarised emission seen in this study suggested possible spiral structure to the overall magnetic field, but uncorrelated with the spiral arms seen in $H\alpha$ and in the mid-infrared. There was no evidence for the pan-Magellanic field suggested by optical data. An important caveat to these results is that Klein et al. (1993) assumed that Faraday rotation toward the LMC was small, and so did not correct for such effects.

3 New Observations

The LMC was surveyed in H I by Kim et al. (1998, 2003), using the Australia Telescope Compact Array (ATCA). These observations involved approximately 1300 pointings at a wavelength of 21 cm, the resulting image being sensitive to all spatial scales in the range $1'$ to $30'$. The advantage of the ATCA is that for this and many other H I experiments, the correlator simultaneously produced full multi-channel (14×8 -MHz) continuum polarimetry in an adjacent frequency band. We have extracted these data from the archive and have analysed the continuum component. The resulting polarisation data form an incredible resource for studying the LMC’s magnetism at unprecedented sensitivity (≈ 0.2 mJy beam $^{-1}$) and resolution ($\approx 40''$).

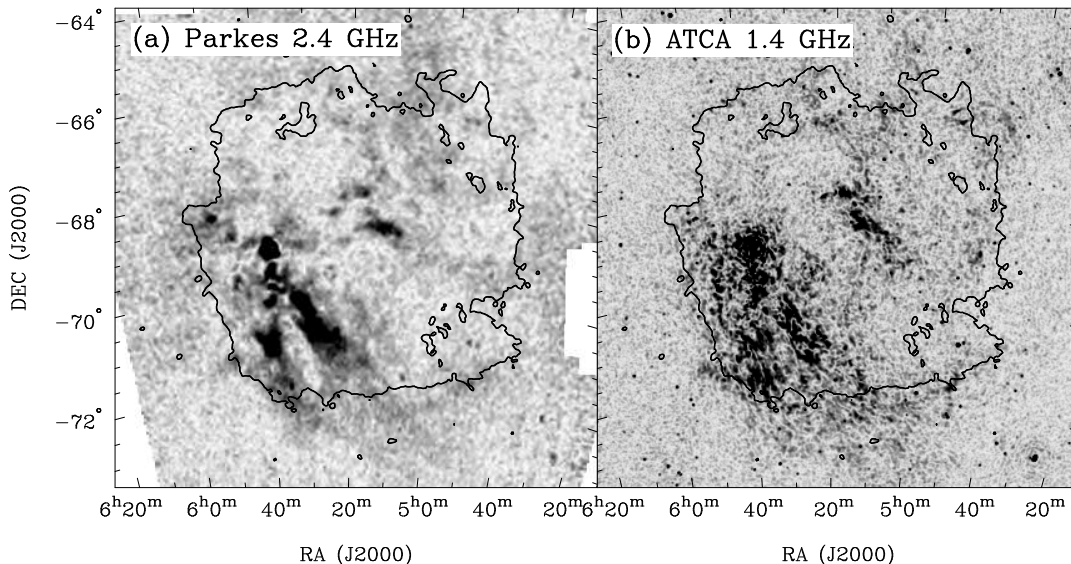


Figure 1: Linearly polarised radio emission from the LMC: (a) 2.4 GHz emission mapped by Parkes, smoothed to a resolution of $30'$ (Klein et al. 1993); (b) 1.4 GHz emission mapped by the ATCA, smoothed to a resolution of $3'$. In both cases, the contour represents *IRAS* $60\text{-}\mu\text{m}$ emission at the level of 1 MJy sr $^{-1}$, delineating the outer boundary of the LMC.

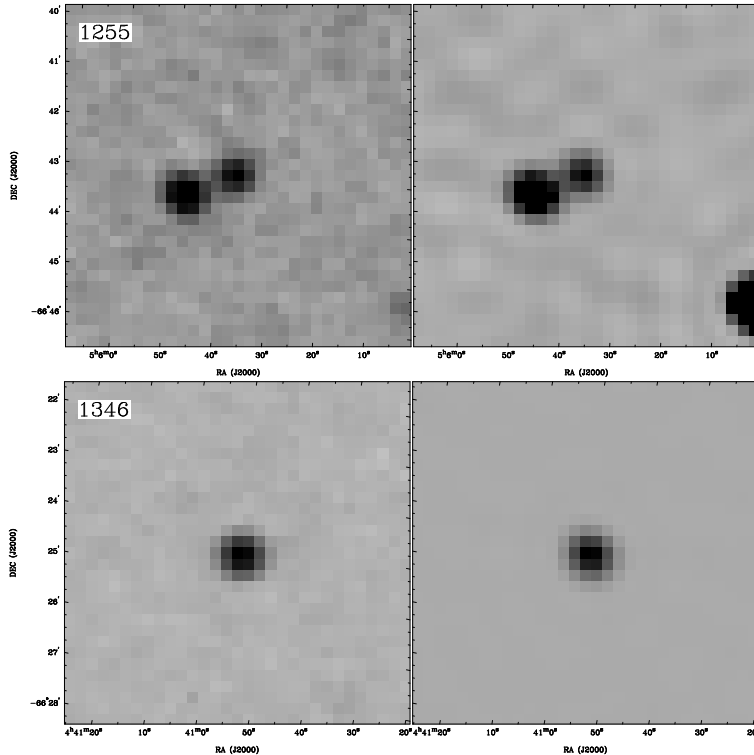


Figure 2: Examples of linear polarisation from background sources in our LMC survey. In each case, the left panel shows the linearly polarised intensity, while the right panel shows the total intensity (the intensity ranges are on different scales for each panel).

4 Results

In Figure 1(b) we show the resulting image of diffuse emission (note that this image comes from an interferometer, and so is not sensitive to structure on scales larger than $\sim 30'$). The two fingers seen with Parkes by Klein et al. (1993) are clearly apparent in our new data. The rest of the polarised emission from the LMC is comprised of possible filaments and shells of emission, showing little correspondence with radio continuum, $H\alpha$, HI or mid-infrared emission. These data will be fully discussed elsewhere; clearly they indicate a complicated mixture of polarised emission and depolarisation, as we have previously seen in our on-going studies of our own Milky Way (e.g., Gaensler et al. 2001; Haverkorn, Katgert, & de Bruyn 2003).

The image shown in Figure 1(b) also demonstrates the existence of linearly polarised emission from approximately 380 unresolved background sources, examples of which are shown in Figure 2. The typical polarised fraction from such sources is $\sim 3\%$, although the faintest sources have higher polarised fractions than this due to sensitivity bias. While the total intensity image can be a complicated mix of diffuse emission, SNRs and H II regions, confusion from diffuse emission is negligible in the polarised image, so that even faint polarised sources can be easily identified (the image in Fig. 1[b] has been significantly smoothed).

For each source, we obtain a measurement of the Stokes parameters Q and U in 14 independent channels centred on 1384 MHz. Because these channels are closely spaced, we do not suffer from the usual $n\pi$ ambiguities present in Faraday rotation measurements provided that RMs have magnitudes less than $\sim 2700 \text{ rad m}^{-2}$ (see Gaensler et al. 1998). For each frequency channel on each source, we consider polarisation position angles for nine adjacent pixels. We fit across the observing band for the RM, and then apply criteria for extent of the source, signal-to-noise, quality of the fit, and pixel-to-pixel scatter in the RMs (e.g., Brown, Taylor, & Jackel 2003). After all these tests were applied, we obtained 292 accurate and reliable RMs in the field of the LMC, at a source density of ~ 2.2 measurements per square degree.

The resulting distribution of RMs is shown in Figure 3, from which a mean baseline RM has been subtracted from the data. There is a clear excess of Faraday rotation toward the LMC, demonstrating the presence of a significant line-of-sight component to the LMC magnetic field. The baseline-subtracted RMs through the LMC have a mean of $+10 \text{ rad m}^{-2}$, but with a large scatter, values ranging from -215 to $+247 \text{ rad m}^{-2}$. These RMs imply large rotations of polarisation position angle in the data of Klein et al. (1993), casting doubt on the validity of the magnetic field geometry that those authors inferred.

5 Discussion

5.1 The Coherent Magnetic Field

We assume that the LMC disk is inclined to the plane of the sky by 35° , with its line of nodes oriented at a position angle of 120° , north through east (van der Marel 2004). With this orientation, the LMC RMs shown in Figure 3 can be shown to trace a sinusoidal pattern as a function of position angle within the LMC's disk, implying a vertically symmetric spiral magnetic field of mode $m = 0$. The pitch angle is difficult to constrain, but is likely to be reasonably low, $\lesssim 20^\circ$. The amplitude of our sinusoidal fit is 53 rad m^{-2} , while the equivalent dispersion measure, as inferred from observations of LMC radio pulsars (Crawford et al. 2001), is $\approx 100 \text{ pc cm}^{-3}$. The implied strength of the uniform field component in the LMC is $\approx 1.1 \mu\text{G}$. This is likely to underestimate the true field strength by a factor of ~ 2 , due

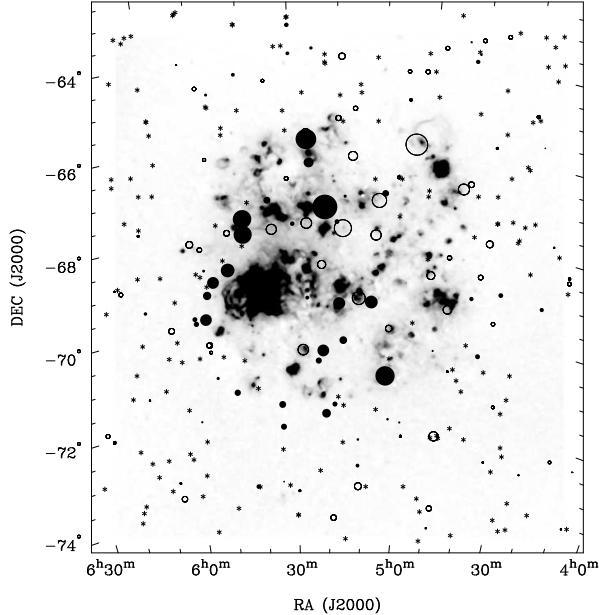


Figure 3: Distribution of RMs behind the LMC (Gaensler et al. 2005). The greyscale denotes emission measures derived from the SHASSA $H\alpha$ survey (Gaustad et al. 2001), while the closed and open circles represent positive and negative RMs, respectively. Asterisks indicate RMs that are consistent with zero within their errors.

to biases induced by correlations between electron density and magnetic field fluctuations in interstellar gas (Beck et al. 2003).

5.2 The Random Magnetic Field

In addition to the coherent field, Figure 3 suggests the presence of significant fluctuations in RM from point to point — the standard deviation in RM over the LMC is 81 rad m^{-2} . On large scales, a structure function analysis reveals a clear outer scale to RM fluctuations at a scale of $\sim 100 \text{ pc}$. This may represent the characteristic scale for the shells and bubbles of ionised gas which dominate the LMC’s morphology as seen in $\text{H}\alpha$ (e.g., Meaburn 1980). We will show in a forthcoming paper that these measurements imply a ratio of random to ordered magnetic field strengths on large scales of ≈ 3.6 , so that the random field dominates the ordered field.

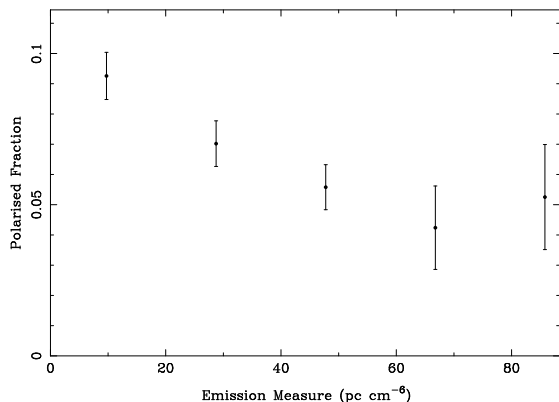


Figure 4: Average polarised fraction vs. emission measure for polarised sources behind the LMC.

polarised fraction vs. foreground emission measure (EM) for sources behind the LMC. As shown in Figure 4, a clear trend is apparent, such that sources behind high EMs seem to be increasingly depolarised.

For these observations this effect can only be due to beam depolarisation, implying large fluctuations in RM on scales smaller than the angular sizes of our sources. All our sources are unresolved, so we must appeal to source statistics (e.g., Windhorst et al. 1993). From such studies we estimate a median angular size for our sample of $\approx 6''$, or $\approx 1.5 \text{ pc}$ at the distance of the LMC. Significant RM fluctuations on scales $\ll 1.5 \text{ pc}$ are implied. In a forthcoming paper, we show that the observed depolarisation can be explained by a random field of strength $5 \mu\text{G}$ on scales of $\sim 0.5 \text{ pc}$. These large field fluctuations do not seem to be part of the standard turbulent cascade from large scales, but rather seem to trace a separate source of fluctuations on sub-parsec scales. Similar small-scale turbulence is seen in RM measurements in our own Galaxy, and possibly delineates the effects of individual stars and H II regions on interstellar gas (e.g., Haverkorn et al. 2004).

Fluctuations in RM on much smaller scales are implied by the fact that polarised sources seem to avoid bright $\text{H}\alpha$ regions in Figure 3. At a quantitative level, the brightest foreground $\text{H}\alpha$ intensity against which we obtain an RM is $\approx 75 \text{ rayleighs}$, even though 7% of all $\text{H}\alpha$ pixels within the boundaries of the LMC are brighter than this. About 90 of our RMs lie directly against the LMC. If these sources are randomly distributed, the probability of having none of them lie behind more than 75 rayleighs of $\text{H}\alpha$ sources is $(1 - 0.07)^{90} \approx 1.5 \times 10^{-3}$. Another way of looking at this effect is to plot

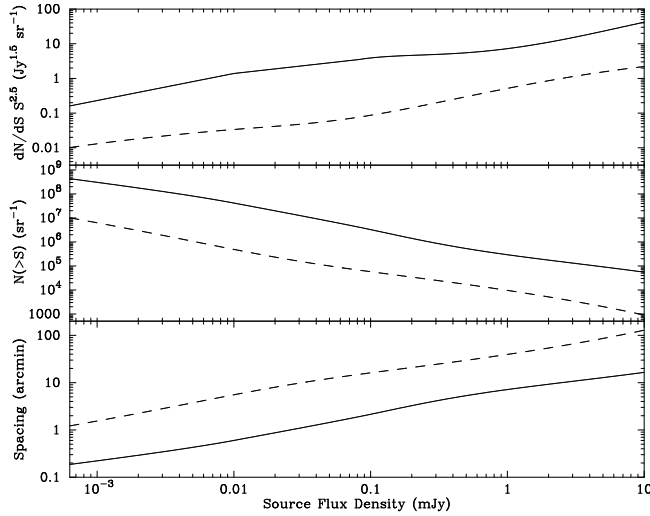


Figure 5: Distribution of extragalactic source counts in both total intensity (solid line) and in linear polarisation (dashed line) at an observing frequency of 1.4 GHz (Beck & Gaensler 2004). The upper, middle and lower panels show the predicted distribution of differential source counts, integral source counts, and mean spacing between sources, respectively. Surveys with current telescopes have a detection threshold of ~ 1 mJy, corresponding to a density of RM measurements of ~ 1 sources deg^{-2} . An all-sky SKA survey will detect sources down to ~ 1 μJy , corresponding to ~ 1500 RMs deg^{-2} .

6 Future RM Experiments with the SKA

The work presented above is a preview of the approach to magnetic field studies that will be routine with the Square Kilometre Array (SKA), a next-generation radio telescope currently being developed by the international community.

“The Origin and Evolution of Cosmic Magnetism” has been named one of five key science projects for the SKA (Gaensler et al. 2004). It is correspondingly highly likely that early in its operations, the SKA will undertake an all-sky continuum survey, providing images of linear polarisation at 1.4 GHz and at arcsecond resolution down to a sensitivity of ≈ 0.1 μJy . Among many exciting applications, this survey will yield RMs from $\sim 2 \times 10^7$ polarised extragalactic radio sources (Beck & Gaensler 2004). From our prediction of the distribution of source counts (see Fig. 5), we expect that RMs will be distributed on the sky at a mean spacing of only $\sim 90''$ between sources!

The resulting “RM grid” will be a fantastic resource for probing magnetic fields in all manner of foreground sources. For the LMC we can expect in excess of 10^5 background RMs, while we will obtain thousands of RMs for many other nearby galaxies and clusters, in dramatic contrast to the handful of RMs available for such sources now (e.g., Han et al. 1998; Govoni et al. 2001).

On larger scales, this RM grid can be used to map the magnetic field of the intergalactic medium (IGM) and of the overall Universe. Magnetic fields from the IGM, although yet to be detected, are likely to act as the seed fields for galaxies and clusters, and may trace or even regulate the formation of structure on large scales. Presently there are dozens of models for

the origin and distribution of IGM magnetic fields, each model potentially making a different prediction for the power spectrum of fluctuations in this large-scale field (for recent reviews see Grasso & Rubinstein 2001; Widrow 2002; Giovannini 2004).

Faraday rotation can potentially detect and map the magnetic field of the IGM, but at the moment only upper limits have been obtained, at the level of 10^{-8} to 10^{-9} G (Kronberg 1994; Blasi, Burles, & Olinto 1999). Since comoving electron densities and magnetic fields both increase in magnitude as a function of redshift, a survey which can accumulate a large sample of RMs from high-redshift sources can potentially detect the RM signature of the IGM (Kolatt 1998). The SKA, in conjunction with optical data from experiments such as LSST or SkyMapper, will have the necessary sensitivity to make these measurements, ultimately yielding the magnetic power spectrum of the observable Universe.

7 Conclusions

Our main results are as follows:

- The LMC has a coherent magnetic field with a spiral geometry, and of strength $\gtrsim 1 \mu\text{G}$.
- On large ($\gtrsim 100$ pc) scales, there is also a significant random component to the magnetic field, which dominates the ordered component by a factor of ~ 3 .
- On small ($\ll 1$ pc) scales, there are strong spatial fluctuations in rotation measure.

We next plan to interpret the diffuse polarised emission from the LMC seen in Figure 1(b). We also have recently obtained corresponding ATCA data on the SMC and on part of the Magellanic Bridge, to which we can apply a similar analysis to that presented here.

This work clearly demonstrates that background RMs, when obtained at sufficiently high density on the sky, can be an exciting and insightful way of mapping magnetic fields. With the advent of the SKA, this will likely become a standard technique for studying magnetism at all distances.

We thank the organisers for running a particularly stimulating and enjoyable conference. We are grateful to Sungeun Kim for carrying out the original ATCA observations which made this project possible. The Southern H-Alpha Sky Survey Atlas (SHASSA) is supported by the National Science Foundation. The Australia Telescope is funded by the Commonwealth of Australia for operation as a National Facility managed by CSIRO. B.M.G. acknowledges the support of the National Science Foundation through grant AST-0307358, and of the University of Sydney through the Denison Fund.

References

- Beck, R. & Gaensler, B. M. 2004, *New Astronomy Reviews*, 48, 1289.
- Beck, R., Shukurov, A., Sokoloff, D., & Wielebinski, R. 2003, *A&A*, 411, 99.
- Blasi, P., Burles, S., & Olinto, A. V. 1999, *ApJ*, 514, L79.
- Brown, J. C., Taylor, A. R., & Jackel, B. J. 2003, *ApJS*, 145, 213.
- Chi, X. & Wolfendale, A. W. 1993, *Nature*, 362, 610.

- Costa, M. E., McCulloch, P. M., & Hamilton, P. A. 1991, *MNRAS*, 252, 13.
- Crawford, F., Kaspi, V. M., Manchester, R. N., Lyne, A. G., Camilo, F., & D'Amico, N. 2001, *ApJ*, 553, 367.
- Gaensler, B. M., Beck, R., & Feretti, L. 2004, *New Astronomy Reviews*, 48, 1003.
- Gaensler, B. M., Dickey, J. M., McClure-Griffiths, N. M., Green, A. J., Wieringa, M. H., & Haynes, R. F. 2001, *ApJ*, 549, 959.
- Gaensler, B. M., Haverkorn, M., Staveley-Smith, L., Dickey, J. M., McClure-Griffiths, N. M., Dickel, J. R., & Wolleben, M. 2005, *Science*, 307, 1610.
- Gaensler, B. M., Manchester, R. N., & Green, A. J. 1998, *MNRAS*, 296, 813.
- Gaustad, J. E., McCullough, P. R., Rosing, W., & Van Buren, D. 2001, *PASP*, 113, 1326.
- Giovannini, M. 2004, *Int. J. Mod. Phys. D*, 13, 391.
- Govoni, F., Taylor, G. B., Dallacasa, D., Feretti, L., & Giovannini, G. 2001, *A&A*, 379, 807.
- Grasso, D. & Rubinstein, H. R. 2001, *Phys. Rep.*, 348, 163.
- Han, J. L., Beck, R., & Berkhuijsen, E. M. 1998, *A&A*, 335, 1117.
- Haverkorn, M., Gaensler, B. M., McClure-Griffiths, N. M., Dickey, J. M., & Green, A. J. 2004, *ApJ*, 609, 776.
- Haverkorn, M., Katgert, P., & de Bruyn, A. G. 2003, *A&A*, 403, 1045.
- Kim, S., Staveley-Smith, L., Dopita, M. A., Freeman, K. C., Sault, R. J., Kesteven, M. J., & McConnell, D. 1998, *ApJ*, 503, 674.
- Kim, S., Staveley-Smith, L., Dopita, M. A., Sault, R. J., Freeman, K. C., Lee, Y., & Chu, Y.-H. 2003, *ApJS*, 148, 473.
- Klein, U., Haynes, R. F., Wielebinski, R., & Meinert, D. 1993, *A&A*, 271, 402.
- Klein, U., Wielebinski, R., Haynes, R. F., & Malin, D. F. 1989, *A&A*, 211, 280.
- Kolatt, T. 1998, *ApJ*, 495, 564.
- Kronberg, P. P. 1994, *Rep. Prog. Phys.*, 57, 325.
- Mathewson, D. S. & Ford, V. L. 1970, *ApJ*, 160, L43.
- Meaburn, J. 1980, *MNRAS*, 192, 365.
- Pohl, M. 1993, *A&A*, 279, L17.
- Schmidt, T. 1976, *A&AS*, 24, 357.
- van der Marel, R. P. 2004, in *The Local Group as an Astrophysical Laboratory*, ed. M. Livio, (Cambridge: Cambridge University Press), in press (astro-ph/0404192).
- Visvanathan, N. 1966, *MNRAS*, 132, 423.

Wayte, S. R. 1990, *ApJ*, 355, 473.

Widrow, L. M. 2002, *Reviews of Modern Physics*, 74, 775.

Windhorst, R. A., Fomalont, E. B., Partridge, R. B., & Lowenthal, J. D. 1993, *ApJ*, 405, 498.